Editors' Suggestion

Precision of Protein Thermometry

Michael Vennettilli,[1,2] Soutick Saha,[2] Ushasi Roy,[2,3] and Andrew Mugler[1,2,*]
[1]Department of Physics and Astronomy, University of Pittsburgh, Pittsburgh, Pennsylvania 15260, USA
[2]Department of Physics and Astronomy, Purdue University, West Lafayette, Indiana 47907, USA
[3]Centre for BioSystems Science and Engineering, Indian Institute of Science, Bangalore 560012, India

(Received 4 December 2020; accepted 6 August 2021; published 26 August 2021)

Temperature sensing is a ubiquitous cell behavior, but the fundamental limits to the precision of temperature sensing are poorly understood. Unlike in chemical concentration sensing, the precision of temperature sensing is not limited by extrinsic fluctuations in the temperature field itself. Instead, we find that precision is limited by the intrinsic copy number, turnover, and binding kinetics of temperature-sensitive proteins. Developing a model based on the canonical TlpA protein, we find that a cell can estimate temperature to within 2%. We compare this prediction with *in vivo* data on temperature sensing in bacteria.

DOI: 10.1103/PhysRevLett.127.098102

Cells routinely make decisions based on the temperature of their surroundings. For example, most cells undergo systemic changes in response to a heat or cold shock [1,2]. Some cells initiate a phenotypic response such as virulence when the temperature crosses a particular threshold [3]. Some cells thermotax, or move toward a preferred temperature range [4]. These behaviors are possible because molecular conformations, chemical reaction rates, and various mechanical properties of cells can change dramatically as a function of temperature, and cells have developed many different ways to detect such changes [5–7]. Molecules that participate in the response to temperature changes are called molecular thermometers or thermosensors, and this class includes DNA and various RNA and protein molecules.

Despite detailed knowledge of the molecular mechanisms of temperature sensing in cells, the basic question of what sets the precision of temperature sensing remains largely unexplored. Is the precision limited extrinsically by temperature fluctuations in the surrounding fluid, or intrinsically by properties of the cell's molecular components? Similar questions have been heavily investigated for other types of cell sensing, beginning with Berg and Purcell's analysis of chemical concentration sensing [8], and extending to sensing of concentration gradients [9], concentration ramps [10], multiple ligands [11], material stiffness [12], and fluid flow [13], among others. In most of these cases, extrinsic fluctuations have been found to limit sensory precision, suggesting that cells have evolved sensors that are as precise as physically possible. However, the precision of temperature sensing, and the associated question of extrinsic versus intrinsic limits, has been understudied by comparison.

Early work by Dusenbery shed important light on this problem [14]. Using the two-point correlation function for temperature fluctuations in a homogeneous fluid, Dusenbery estimated that extrinsic fluctuations are several orders of magnitude smaller than cells' actual sensitivity thresholds. This finding suggests that cells' temperature sensors are not as precise as physically possible. However, it leaves an important question unanswered: if extrinsic fluctuations do not set the limit on the precision of cellular temperature sensing, then what does?

Here we revisit this problem from a perspective that combines the physics of temperature fluctuations with the molecular mechanisms of thermoreception. Following Dusenbery's lead, we start by using the two-point correlation function to investigate a thermal analog of Berg and Purcell's "perfect instrument" for concentration sensing [8]. This investigation confirms that extrinsic temperature fluctuations are far too small to be limiting in a biological context. We therefore investigate the intrinsic fluctuations imposed by cells' molecular machinery for temperature sensing. We are guided by a prototypical and well studied protein thermometer, namely the TlpA protein in the bacterium *Salmonella typhimurium* [15–17]. Developing a stochastic model based on the experimentally characterized details of TlpA, we find that intrinsic fluctuations are much larger than extrinsic fluctuations and can in fact be biologically limiting. Specifically, we find that intrinsic fluctuations impose a sensing error of roughly 2%, and we discuss how this limit compares with the observed temperature sensing threshold in bacteria.

In their perfect instrument for concentration sensing, Berg and Purcell considered a completely permeable sphere of radius a that could count the number of molecules within its volume at each instant, perform a time average, and use this information to estimate the surrounding concentration [8]. In the case of temperature sensing, the analogous instrument is a permeable sphere of radius a that records the temperature $T(\vec{x}, t)$ at each point within its volume at each instant $t \in [0, \tau]$, performs a volume and time average,

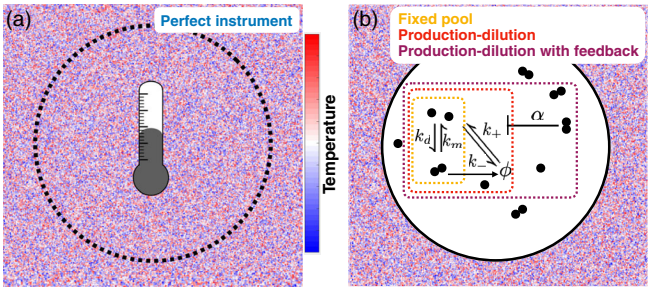

FIG. 1. Temperature sensing (a) via an analog of Berg and Purcell's [8] perfect instrument for concentration sensing, and (b) via a protein thermometer. Based on the TlpA protein, monomers reversibly dimerize, monomers are expressed, monomer and dimers are diluted by cell division, and dimers inhibit monomer expression.

and then uses the result as the temperature estimate $\hat{T}$ [Fig. 1(a)]. We assume the medium to be homogeneous and in thermal equilibrium, with average temperature $\bar{T}$. The key ingredient is the two-point correlation function for the temperature fluctuations obtained in the regime of linear irreversible thermodynamics [18]

$$\langle [T(\vec{x},t)-\bar{T}][T(\vec{x}',t')-\bar{T}]\rangle = \frac{k_B\bar{T}^2}{\rho c_s}\left(\frac{\rho c_s}{4\pi K|t-t'|}\right)^{3/2}\exp\left[-\frac{\rho c_s\|\vec{x}-\vec{x}'\|^2}{4K|t-t'|}\right], \quad (1)$$

where k_B is Boltzmann's constant and the material properties ρ, c_s, and K are the mass density, specific heat, and thermal conductivity of the medium, respectively. The variance in the estimator is computed by integrating the two-point correlation function in Eq. (1) in both space and time. The result has the following short- and long-time limits [19],

$$\frac{\sigma(\hat{T})}{\bar{T}} = \sqrt{\frac{k_B}{C}}\times\begin{cases}1 & \tau\to 0\\ \sqrt{4\tau_D/(5\tau)} & \tau\gg\tau_D,\end{cases} \quad (2)$$

where we have introduced the heat capacity of the medium contained within the instrument $C=4\pi a^3\rho c_s/3$ and the timescale for temperature fluctuations to diffuse across the instrument $\tau_D=\rho c_s a^2/K$ [18]. Equation (2) has an intuitive interpretation: the variance falls off with the heat capacity of the instrument (in units of k_B) because if the heat capacity is large, a large fluctuation in thermal energy corresponds to a small fluctuation in temperature. The variance is further decreased in the long-time limit by the number τ/τ_D of independent measurements the instrument can make, where independence is defined by the diffusion time.

For water at room temperature, $\rho\approx 1$ g/cm^3, $c_s\approx 4$ J/(g · K), and $K\approx 0.6$ J/(s · m · K). For a cell radius of $a\approx 1$ μm, the error in an instantaneous measurement according to Eq. (2) is $\sigma(\hat{T})/\bar{T}\approx 10^{-6}$. The diffusion time

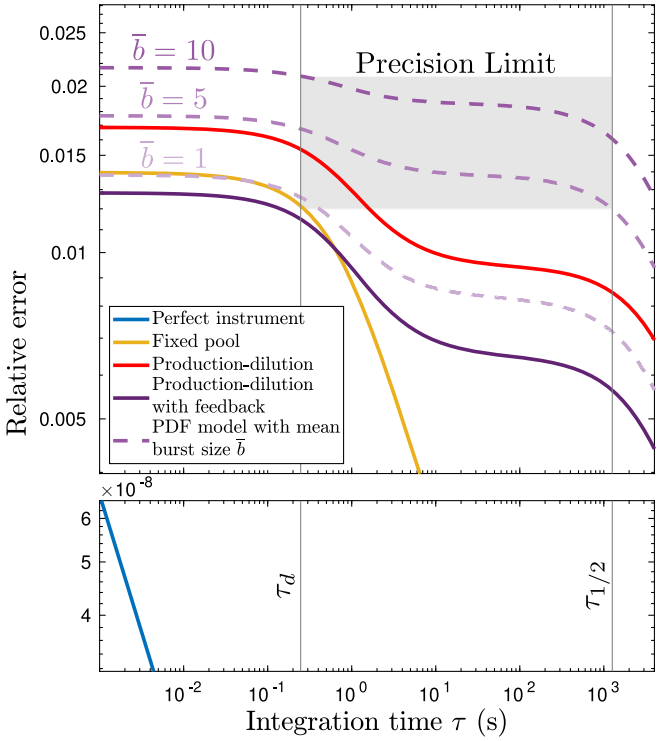

FIG. 2. Relative temperature estimation error $\sigma(\hat{T})/\Delta T$ as a function of monomer-number integration time τ. We predict that the error is bounded from below by 2% (gray box). Parameters are estimated from data as described in the text.

is $\tau_D\approx 6$ μs, after which the error drops further due to time averaging (Fig. 2, blue). Clearly the extrinsic fluctuations in the medium itself are not limiting, as it is unlikely that a cell needs to estimate temperature to less than one part in a million. This finding agrees with the conclusions of Dusenbery, whose approach was more heuristic [14].

Of course, cells are not perfect thermometers. They detect temperature indirectly through molecular or mechanical properties [5–7]. Therefore, to investigate the intrinsic limits imposed by the detection mechanism itself, we must develop a model that accounts for the information actually available to the cell. Here we focus on the molecular mechanism of protein thermometry, in which proteins' conformational states are temperature dependent. Protein thermometers are ubiquitous: for example, temperature-dependent oligomerization, unfolding or misfolding, and methylation of proteins drive, in various combinations, the heat shock response [1], high-temperature response [17,20], and thermotaxis response [4,21,22] in bacteria. In these cases, a temperature-induced conformational change is generally followed by negative feedback [23].

For concreteness, we consider the protein TlpA in *S. typhimurium*, which includes these common features but is otherwise relatively simple and experimentally well characterized. A step in temperature results in a sustained, rather than transient, new TlpA level, suggesting that TlpA responds to absolute temperature rather than temperature

change [19]. TlpA forms homodimers, with the dimer favored at low temperatures and the monomer favored at high temperatures [15,17]. The dimer binds to the promoter region of the *tlpA* gene and inhibits its expression [16], resulting in negative feedback. TlpA is a canonical protein thermometer, and its mechanism has been used to engineer other thermal switches [24,25].

Suppose that two TlpA molecules associate with rate k_d and dissociate with rate k_m [15] [Fig. 1(b), yellow]. Subject to these reactions alone, the total number of TlpA units $n = m + 2d$ is conserved, where m and d are the numbers of monomers and dimers, respectively. Therefore we refer to this as the "fixed pool" (FP) model. The mean fraction $f = \bar{m}/n$ of TlpA units in the monomeric state has been measured as a function of temperature at physiological concentrations using circular dichroism spectroscopy [17,26]. We find that the data are well described by a sigmoid $f(T) = \{1 + \exp[-4(T - T_M)/\Delta T]\}^{-1}$ with half-maximal temperature $T_M = 39\,°\mathrm{C}$ and width $\Delta T = 6.3\,°\mathrm{C}$ [19] [the factor of 4 ensures that $f'(T_M) = 1/\Delta T$]. We assume that the cell infers the temperature from the mean monomer number, which it estimates from the time average $\hat{m}_\tau = \tau^{-1}\int_0^\tau m(t)dt$ [8] (we find similar results if temperature is instead inferred from the dimer number [19]). In the Supplemental Material [19] we also consider maximum likelihood estimation [27], which in this case has the least squared error of all possible estimators, and find that it performs similarly to the naive time average considered here.

To convert the error in monomer number estimation to that in temperature estimation, we use linear error propagation [8], $\sigma(\hat{T}) = \sigma(\hat{m}_\tau)/|d\bar{m}/dT| = \sigma(\hat{m}_\tau)/(nf')$, where the second step follows from $\bar{m} = nf$. To find $\sigma(\hat{m}_\tau)$, we perform the second-order Kramers-Moyal expansion and linearize to obtain the fluctuations [28–30]. The result is [19]

$$\frac{\sigma(\hat{T})}{\Delta T} = \frac{\sigma_{\mathrm{FP}}(m)}{nf'\Delta T} \times \begin{cases} 1 & \tau \to 0 \\ \sqrt{2\tau_d/\tau} & \tau \gg \tau_d, \end{cases} \tag{3}$$

where $\sigma^2_{\mathrm{FP}}(m) = 2nf(1-f)/(2-f)$ is the instantaneous variance in the monomer number and $\tau_d = c(k_d\bar{m})^{-1}$ is the autocorrelation time, with $c = (1-f)/[2(2-f)]$ a numerical factor [31]. Equation (3) has an intuitive interpretation: the factor $nf(1-f)$ in $\sigma^2_{\mathrm{FP}}(m)$ is the variance of the binomial distribution, which arises because the molecules switch between the monomer and dimer states. The additional factor $2/(2-f)$ is an increase in the noise due to the fact that dimerization further discretizes the monomer number beyond that of a pure binomial process, as the monomer number can only change by two [32]. Finally, $(k_d\bar{m})^{-1}$, which sets τ_d, is the timescale for a monomer to form a dimer with any other monomer. As in Eq. (2), the variance in the long-time limit of Eq. (3) is reduced by the number τ/τ_d of independent measurements made.

When $T = T_M$, we have $f = 1/2$ and $f' = 1/\Delta T$, and the instantaneous error in Eq. (3) reduces to $\sigma(\hat{T})/\Delta T = 1/\sqrt{3n}$. We see that the error decreases with the square root of the number of TlpA molecules n, as expected for counting noise. From the experimentally estimated number of TlpA dimers per cell [17], we infer $n \approx 1700$ [33], and therefore an instantaneous error of $\sigma(\hat{T})/\Delta T = 1.4\%$ (Fig. 2, yellow). To see how sensing improves with time integration, we need to estimate the dimerization rate k_d. We are unaware of an experimental estimate for the dimerization rate of TlpA. However, TlpA is a coiled coil, and the dimerization rate of engineered coiled coils has been measured at $k_d V = 4 \times 10^5\ (\mathrm{M}\cdot\mathrm{s})^{-1}$ [34]. Given the bacterial volume of $V = 1\ \mu\mathrm{m}^3$ [35], this results in an autocorrelation time of $\tau_d = 0.3$ s at $f = 1/2$, beyond which the error falls off [36]. The intrinsic noise from molecular detection (Fig. 2, yellow) clearly dominates over the extrinsic noise from temperature fluctuations in the medium (Fig. 2, blue).

The fixed pool model is unrealistic because in cells the protein number is not actually fixed. Instead, proteins are produced via gene expression and lost by active degradation or dilution from cell division. As we are not aware of evidence that TlpA is actively degraded, we consider dilution here. Specifically, we introduce a production rate k^+ for the monomer and a dilution rate k^- for both the monomer and dimer. We call this the "production-dilution" model [Fig. 1(b), red]. Experiments [17,37] suggest that neither k^+ nor k^- is strongly temperature dependent [19], and therefore we assume that the dominant temperature dependence is via f. Because cell division is much slower than monomer binding [38], we consider the limit $k^- \ll k_d\bar{m}$.

Using the same stochastic techniques as above, we find [19] that the mean and variance of the monomer number become $\bar{m} = fk^+/k^-$ and

$$\sigma^2(m) = \sigma^2_{\mathrm{FP}}(m) + \frac{f^2\sigma^2(n)}{(2-f)^2}, \tag{4}$$

where $\sigma^2(n) = (7-3f)k^+/(4k^-)$ is the variance of the (now fluctuating) pool size $n = m + 2d$, and $\sigma^2_{\mathrm{FP}}(m)$ as given beneath Eq. (3) is here written in terms of the mean pool size $\bar{n} = \bar{m}/f$. The second term in Eq. (4) is always positive, showing that pool fluctuations due to protein turnover increase the noise, as expected. Indeed, using $f = 1/2$ and k^+/k^- inferred from the experimental dimer number [33], we see that the instantaneous error (Fig. 2, red) is increased from that of the FP model (Fig. 2, yellow). The full τ-dependent expression for $\sigma(\hat{T})/\Delta T$ is calculated [36] using $k^- = \ln(2)/\tau_{1/2} \approx 2\ \mathrm{hr}^{-1}$ from cell division [39], and we see that the relative error has two clear bends at the dimerization and dilution timescales τ_d and $\tau_{1/2}$, respectively (Fig. 2, red).

Thus far we have not yet accounted for the fact that TlpA exhibits negative feedback: the TlpA dimer binds to the promoter region of the *tlpA* gene and inhibits its expression [16]. To incorporate this autorepression, we replace the monomer production rate k^+ with the function $k^+/(1+\alpha d)$. We call this the "production-dilution with feedback" (PDF) model [Fig. 1(b), purple]. The parameter α describes the autorepression strength, and its inverse sets where half-maximal expression occurs. Experiments [17] suggest that α is not strongly temperature dependent [19], and therefore we continue to assume that the dominant temperature dependence is via f. With autorepression, we find [19] that the mean monomer number becomes

$$\bar{m} = \frac{f}{\alpha(1-f)}\left[\sqrt{1+\frac{2\alpha k^+(1-f)}{k^-}}-1\right], \tag{5}$$

and the variance obeys Eq. (4) with $\sigma^2(n)$ acquiring an α dependence (see Ref. [19]). We have checked [19] that Eqs. (4) and (5) agree with stochastic simulations [40]. Both Eq. (4) and Eq. (5) decrease monotonically with α, showing that autorepression reduces both the monomer number variance and its mean. The latter effect dominates, such that relative fluctuations $\sigma(m)/\bar{m}$ increase with autorepression strength [41].

The increase in relative fluctuations with autorepression is offset by an increase in temperature sensitivity. To see this, we recognize that the instantaneous relative error can be written $\sigma(\hat{T})/\Delta T = [\sigma(m)/\bar{m}]/[|d\bar{m}/dT|(\Delta T/\bar{m})]$, again by error propagation. The first term in brackets is the relative fluctuations while the second term is the sensitivity: the derivative $d\bar{m}/dT$ scaled by the characteristic quantities $\bar{m}$ and ΔT. Differentiating Eq. (5), the sensitivity evaluates to

$$\frac{d\bar{m}}{dT}\frac{\Delta T}{\bar{m}} = \frac{f'\Delta T}{(1-f)}\left[\frac{1}{f}-\frac{1}{2}-\frac{1}{2\sqrt{1+2\alpha k^+(1-f)/k^-}}\right]. \tag{6}$$

Equation (6) is an increasing function of α, showing that autorepression increases the sensitivity. This result is consistent with the fact that mutations that target the autorepression result in a weakened dependence of monomer number on temperature [17].

The tradeoff between increasing relative fluctuations and increasing sensitivity leads to an optimal autorepression strength $\alpha^* = 1.75k^-/k^+$ that minimizes the error in instantaneous temperature sensing $\sigma(\hat{T})/\Delta T$ at $T = T_M$ [19]. Using this value, $f = 1/2$, $k^- = 2\ \mathrm{hr}^{-1}$, and k^+/k^- inferred from the experimental dimer number [33], we see that the error (Fig. 2, purple solid) [36] is reduced from the case without feedback (Fig. 2, red).

Finally, we account for a ubiquitous source of additional noise in bacterial gene expression, namely, bursts. Bursts of protein production can occur at the transcriptional level, due to binding and unbinding at the promoter region [42], and at the translational level, due to multiple proteins being produced from a single transcript [43]. In our case the promoter binding timescale, assuming it is diffusion limited, is sufficiently fast compared to the protein production timescale that transcriptional bursting can be neglected [19,44,45], and therefore we focus on translational bursts. Specifically, we perform stochastic simulations [40] of the PDF model in which each production event generates b TlpA proteins instead of one, where b is geometrically distributed with mean $\bar{b}$ [43], and we take $k^+ \to k^+/\bar{b}$ to leave the mean monomer number $\bar{m}$ unchanged. We see in Fig. 2 that the temperature estimation error increases with mean burst size $\bar{b}$, as expected (purple dashed).

Our results provide a quantitative prediction for the precision with which a cell can estimate temperature using a protein thermometer. A temperature-sensitive behavioral response is likely to occur on a timescale slower than monomer binding τ_d but faster than cell division $\tau_{1/2}$. Figure 2 shows that the estimation error is relatively insensitive to the integration time in this range. In particular, for a typical bacterial protein burst size of $\bar{b} = 5$–10 molecules [43], we predict that the cell can estimate temperature to within 2% (Fig. 2, gray box).

How does the predicted bound of 2% precision compare to observed thermosensing thresholds in experimental systems? The transcriptional activity of TlpA has been measured *in vivo* [17] using a Miller assay with a LacZ reporter [46,47]. Miller units are proportional to the number of TlpA production events and therefore include time integration while excluding noise downstream of TlpA. Measurements at temperatures T_1 and T_2 below and above the transition temperature, respectively, provide an estimate of the thermosensing error $\sigma(\hat{T})/\Delta T$, where $\Delta T = T_2 - T_1$, and $\sigma(\hat{T})$ is evaluated from the measured uncertainties using linear error propagation (see Ref. [19] for details). Using this procedure, we find $\sigma(\hat{T})/\Delta T = 24\%$. This value is larger than 2%, indicating that this protein thermometer obeys the predicted bound. In fact, modeling the LacZ reporter explicitly, the predicted bound becomes 20%–30% due to the additional reporter noise [19], which is consistent with the experimental observation of 24%.

The excellent agreement between the predicted bound and the experimental observation may be partly fortuitous. First, the data may include purely experimental sources of error associated with the Miller assay, which would increase the observed error. Second, the Miller assay is a population measurement, which would decrease the observed error: it reports $[\sigma(\hat{T})/\Delta T]/\sqrt{N}$, where N is the number of independently responding units within the population of N_{cells}, and the degree to which cells respond in a correlated ($N \to 1$) or uncorrelated ($N \to N_{\mathrm{cells}}$) manner is unclear. Third, the population likely includes natural cell-to-cell variability [48], which would increase

the observed error. These unknowns underscore the need for measurements of temperature sensitivity at the single-cell level. We are not aware of any such measurement for a protein thermometer.

Molecular thermometers drive a variety of cell behaviors, and it is natural to ask how our work could be extended. Many thermosensors, including TlpA, are speculated to cause thresholdlike responses, where the cell cares only if the temperature is above a particular threshold, not the value of the temperature itself. For this task, decision theory or optimal stopping [49–51] may be more appropriate than the time-integrated statistics we investigate here. Furthermore, many thermosensors are used for thermotaxis, the motion of a cell toward an optimal temperature. Here the sensory network is more complicated [21,22] and the task is also different: the cell cares about the value of both the temperature and its spatial gradient. It would be interesting to integrate our findings into a model of thermotaxis to investigate the physical limits to the precision of that behavior.

Guided by a canonical protein thermometer, we have derived the physical limits to the precision of cellular temperature sensing. Unlike for many other types of cell sensing, the precision of temperature sensing is evidently not limited by the extrinsic noise inherent to the environmental signal itself. Instead, the precision is limited by the biochemical details of the molecular thermometer inside the cell. Specifically, the relative error falls off with the square root of the number of molecules and the number of correlation times, as expected for systems dominated by biochemical noise. Developing a model based on the experimental features and measured parameters of the TlpA protein, we predict a sensitivity threshold of 2%, which we find is consistent with the observed thermosensing threshold in bacteria. Our work advances the understanding of cell sensing and lays the groundwork for further exploration of temperature-sensitive cell behavior.

This work was supported by the Simons Foundation (376198) and the National Science Foundation (PHY-1945018).

*andrew.mugler@pitt.edu

[1] J. S. McCarty and G. C. Walker, DnaK as a thermometer: Threonine-199 is site of autophosphorylation and is critical for ATPase activity, Proc. Natl. Acad. Sci. U.S.A. **88**, 9513 (1991).

[2] K. Zhao, M. Liu, and R. R. Burgess, The global transcriptional response of escherichia coli to induced σ32 protein involves σ32 regulon activation followed by inactivation and degradation of σ32 *in vivo*, J. Biol. Chem. **280**, 17758 (2005).

[3] M. Falconi, B. Colonna, G. Prosseda, G. Micheli, and C. O. Gualerzi, Thermoregulation of Shigella and Escherichia coli EIEC pathogenicity, A temperature-dependent structural transition of DNA modulates accessibility of virF promoter to transcriptional repressor H-, EMBO J. **17**, 7033 (1998).

[4] K. Maeda, Y. Imae, J. I. Shioi, and F. Oosawa, Effect of temperature on motility and chemotaxis of Escherichia coli, J. Bacteriol. **127**, 1039 (1976).

[5] W. Schumann, Thermosensors in eubacteria: Role and evolution, J. Biosci. **32**, 549 (2007).

[6] B. Klinkert and F. Narberhaus, Microbial thermosensors, Cell Mol. Life Sci. **66**, 2661 (2009).

[7] P. Mandin and J. Johansson, Feeling the heat at the millennium: Thermosensors playing with fire, Mol. Microbiol. **113**, 588 (2020).

[8] H. C. Berg and E. M. Purcell, Physics of chemoreception, Biophys. J. **20**, 193 (1977).

[9] R. G. Endres and N. S. Wingreen, Accuracy of direct gradient sensing by single cells, Proc. Natl. Acad. Sci. U.S.A. **105**, 15749 (2008).

[10] T. Mora and N. S. Wingreen, Limits of Sensing Temporal Concentration Changes by Single Cells, Phys. Rev. Lett. **104**, 248101 (2010).

[11] T. Mora, Physical Limit to Concentration Sensing Amid Spurious Ligands, Phys. Rev. Lett. **115**, 038102 (2015).

[12] F. Beroz, L. M. Jawerth, S. Mnster, D. A. Weitz, C. P. Broedersz, and N. S. Wingreen, Physical limits to biomechanical sensing in disordered fibre networks, Nat. Commun. **8**, 16096 (2017).

[13] S. Fancher, M. Vennettilli, N. Hilgert, and A. Mugler, Precision of Flow Sensing by Self-Communicating Cells, Phys. Rev. Lett. **124**, 168101 (2020).

[14] D. B. Dusenbery, Limits of thermal sensation, J. Theor. Biol. **131**, 263 (1988).

[15] P. Koski, H. Saarilahti, S. Sukupolvi, S. Taira, P. Riikonen, K. Osterlund, R. Hurme, and M. Rhen, A new alpha-helical coiled coil protein encoded by the Salmonella typhimurium virulence plasmid, J. Biol. Chem. **267**, 12258 (1992).

[16] R. Hurme, K. D. Berndt, E. Namork, and M. Rhen, DNA binding exerted by a bacterial gene regulator with an extensive coiled-coil domain, J. Biol. Chem. **271**, 12626 (1996).

[17] R. Hurme, K. D. Berndt, S. J. Normark, and M. Rhen, A proteinaceous gene regulatory thermometer in Salmonella, Cell **90**, 55 (1997).

[18] R. F. Fox, Gaussian stochastic processes in physics, Phys. Rep. **48**, 179 (1978).

[19] See Supplemental Material at http://link.aps.org/supplemental/10.1103/PhysRevLett.127.098102 for additional derivations, experimental data analysis, and simulation results.

[20] P. Servant, C. Grandvalet, and P. Mazodier, The RheA repressor is the thermosensor of the HSP18 heat shock response in Streptomyces albus, Proc. Natl. Acad. Sci. U.S.A. **97**, 3538 (2000).

[21] L. Jiang, Q. Ouyang, and Y. Tu, A mechanism for precision-sensing via a gradient-sensing pathway: A model of Escherichia coli thermotaxis, Biophys. J. **97**, 74 (2009).

[22] A. Paulick, V. Jakovljevic, S. Zhang, M. Erickstad, A. Groisman, Y. Meir, W. S. Ryu, N. S. Wingreen, and V. Sourjik, Mechanism of bidirectional thermotaxis in Escherichia coli, eLife **6**, e26607 (2017).

[23] In the high temperature response, the negative feedback is due to transcriptional repression, for example, via dimers repressing monomer production as discussed herein; in the heat shock response, it is due to proteases degrading or chaperones conformationally changing the oligomers that form [1]; in *E. coli* thermotaxis, it is due to the methylation of the receptors [21,22].

[24] D. I. Piraner, M. H. Abedi, B. A. Moser, A. Lee-Gosselin, and M. G. Shapiro, Tunable thermal bioswitches for *in vivo* control of microbial therapeutics, Nat. Chem. Biol. **13**, 75 (2017).

[25] D. I. Piraner, Y. Wu, and M. G. Shapiro, Modular thermal control of protein dimerization, ACS Synth. Biol. **8**, 2256 (2019).

[26] M. P. Heyn and W. O. Weischet, Circular dichroism and fluorescence studies on the binding of ligands to the subunit of tryptophan synthase, Biochemistry **14**, 2962 (1975).

[27] T. M. Cover and J. A. Thomas, *Elements of Information Theory* (John Wiley & Sons, New York, 2012).

[28] N. G. Van Kampen, *Stochastic Processes in Physics and Chemistry* (Elsevier, New York, 2011).

[29] C. Gardiner, *Stochastic Methods: A Handbook for the Natural and Social Sciences* (Springer Berlin Heidelberg, Berlin Heidelberg, 2009).

[30] F. C. Klebaner, *Introduction To Stochastic Calculus With Applications* (World Scientific Publishing Company, Singapore, 2012).

[31] A cell must be able to determine temperature changes to a better precision than the width of its temperature sensitive region ΔT. For this reason, we define relative error with respect to ΔT, not the mean temperature $\bar{T}$, in Eq. (3) and thereafter. This is in contrast to the case of the perfect instrument [Eq. (2)], for which there is no cell-defined temperature-sensitive region. It is worth noting that even if $\bar{T}$ were replaced with ΔT in Eq. (2), the relative error would increase by roughly 2 orders of magnitude, which is still far less than that of the biochemical models considered in this work.

[32] E. Roob, N. Trendel, P. R.e, and A. Mugler, Cooperative clustering digitizes biochemical signaling and enhances its fidelity, Biophys. J. **110**, 1661 (2016).

[33] The TlpA dimer number was experimentally estimated to be $\bar{d} = 684$ at $T = 37\,^{\circ}\mathrm{C}$ [17], where $f = 0.2$. Because $f = \bar{m}/(\bar{m} + 2\bar{d})$, we have $\bar{m} = 2\bar{d}f/(1-f) = 342$. In the fixed pool model, this implies $n = \bar{m}/f = 1710$. In the production-dilution model, this implies $k^+/k^- = \bar{m}/f = 1710$. In the production-dilution with feedback model, we insert $\bar{m} = 342$, $f = 0.2$, and $\alpha = \alpha^* = 1.75k^-/k^+$ into Eq. (5) to obtain $k^+/k^- = 2521$.

[34] H. Chao, D. L. Bautista, J. Litowski, R. T. Irvin, and R. S. Hodges, Use of a heterodimeric coiled-coil system for biosensor application and affinity purification, J. Chromatogr., B: Biomed. Sci. Appl. **715**, 307 (1998).

[35] J. Smit, Y. Kamio, and H. Nikaido, Outer membrane of Salmonella typhimurium: Chemical analysis and freeze-fracture studies with lipopolysaccharide mutants, J. Bacteriol. **124**, 942 (1975).

[36] The expressions for $\sigma(\hat{T})/\Delta T$ vs τ for all models are calculated analytically by matrix inversion in Mathematica. Code is available at https://github.com/MichaelVennettilli/ProteinThermometry.

[37] K. Fehlhaber and G. Krüger, The study of Salmonella enteritidis growth kinetics using rapid automated bacterial impedance technique, J. Appl. Microbiol. **84**, 945 (1998).

[38] R. Milo and R. Phillips, *Cell Biology by the Numbers*, (Garland Science, 2015).

[39] D. B. Lowrie, V. R. Aber, and M. E. Carrol, Division and death rates of Salmonella typhimurium inside macrophages: Use of penicillin as a probe, J. Gen. Microbiol. **110**, 409 (1979).

[40] D. T. Gillespie, Exact stochastic simulation of coupled chemical reactions, J. Phys. Chem. **81**, 2340 (1977).

[41] We find that the relative fluctuations $\sigma(m)/\bar{m}$ scale as $\alpha^{1/4}$ and as $c + s\alpha$ for large and small α, respectively, where c and s are independent of α. For $0 < f < 0.77$, the slope s is positive. Because we are generally concerned with values of f near $1/2$, we conclude that $\sigma(m)/\bar{m}$ increases monotonically for all α.

[42] A. Raj and A. Van Oudenaarden, Nature, nurture, or chance: Stochastic gene expression and its consequences, Cell **135**, 216 (2008).

[43] X. S. Xie, P. J. Choi, G.-W. Li, N. K. Lee, and G. Lia, Single-molecule approach to molecular biology in living bacterial cells, Annu. Rev. Biophys. **37**, 417 (2008).

[44] H. P. Erickson, Size and shape of protein molecules at the nanometer level determined by sedimentation, gel filtration, and electron microscopy, Biol. Proc. Online **11**, 32 (2009).

[45] A. J. Stewart, S. Hannenhalli, and J. B. Plotkin, Why transcription factor binding sites are ten nucleotides long, Genetics **192**, 973 (2012).

[46] J. H. Miller and J. B. Miller, *Experiments in Molecular Genetics*, (Cold Spring Harbor Laboratory, New York, 1972).

[47] H. G. Garcia, H. J. Lee, J. Q. Boedicker, and R. Phillips, Comparison and calibration of different reporters for quantitative analysis of gene expression, Biophys. J. **101**, 535 (2011).

[48] R. Foreman and R. Wollman, Mammalian gene expression variability is explained by underlying cell state, Mol. Syst. Biol. **16**, e9146 (2020).

[49] E. D. Siggia and M. Vergassola, Decisions on the fly in cellular sensory systems, Proc. Natl. Acad. Sci. U.S.A. **110**, E3704 (2013).

[50] J. O. Berger, *Statistical Decision Theory and Bayesian Analysis* (Springer Science & Business Media, New York, 1985).

[51] G. Peskir and A. Shiryaev, *Optimal Stopping and Free-Boundary Problems* (Springer-Verlag, New York, 2006).